Journal of Fluids and Structures 104 (2021) 103294

Contents lists available at ScienceDirect

Journal of Fluids and Structures

journal homepage: www.elsevier.com/locate/jfs

A note on the state space representation of aeroelastic systems for time domain analysis

Douglas D. Bueno [a,*], Earl H. Dowell [b]

[a] São Paulo State University (UNESP), School of Engineering of Ilha Solteira, Department of Mathematics, Ilha Solteira, SP, Brazil
[b] Duke University, Department of Mechanical Engineering and Material Science, Durham, NC, USA

ARTICLE INFO

Article history:
Received 25 February 2020
Received in revised form 6 April 2021
Accepted 13 April 2021
Available online 20 May 2021

Keywords:
State space representation
Time domain analysis
Eigenvalue problem

ABSTRACT

The time domain state space model for describing an aeroelastic system has usually been obtained by using rational function approximations to write unsteady aerodynamics in the time domain. This strategy has been employed by many researchers because the standard form of unsteady aerodynamics is typically computed in the reduced frequency domain with explicit or implied transcendental functions, which do not readily admit to applying frequency to time domain transforms. However, this article demonstrates that the unsteady aerodynamics do not need to be explicitly written in the time domain when the purpose is to obtain a state space model for aeroelastic analysis. A basic and classical result from the linear algebra is employed for constructing a constant dynamic matrix by using the pair of eigenvalues and eigenvectors obtained iteratively from the *pk* method. The results show that the new approach provides accurate results for linear dynamic aeroelastic models described in either physical or generalized coordinates.

The state space representation of a dynamic system is a very convenient mathematical form to rewrite a second order differential equation (DE) system into a first order DE system. Its most important benefits are achieved if this representation is written in the time domain, because it allows one to study nonlinear problems by integrating the system of equations (Harmin and Cooper, 2011). Additionally, it simplifies the use of several methods developed for designing feedback and output-based controllers (Ogata, 1990; Gawronski, 2004), creating state observers (Kalman, 1960; Jo and Seo, 2000), and for system identification (van Overschee and de Moor, 1996; Bernal, 2008; De Jesus-Mota et al., 2009), for example. It is a very convenient form for describing the aeroelastic system, especially for aeroservoelasticity.

Aeroelastic systems have been described by the state space representation for different applications. They involve gust alleviation (Karpel, 1981; Gennaretti and Mastroddi, 2004), the inclusion of uncertainties (Bueno et al., 2015), different types of controllers (Dinu et al., 2005; Mukhopadhyay, 1999), development of reduced order models (Roughen et al., 2009; Gennaretti and Muro, 2012; Gori et al., 2016), also using computational fluid dynamic simulations (Silva and Raveh, 2001), among others. However, for investigating the aeroelastic system in the time domain, commonly previous investigators use rational function approximations to represent the aerodynamics. It is a well-known strategy in the literature, and because of this different methods of approximation have been developed over the years (Roger, 1977; Abel, 1979; Karpel, 1981; Biskri et al., 2006; Marqui et al., 2017).

The methods involve the inclusion of lag states (Roger, 1977; Abel, 1979; Karpel, 1981; Biskri et al., 2006), or the definition of a number of terms to truncate a polynomial-based series (Marqui et al., 2017). They are developed for describing the unsteady aerodynamic forces for general applications in dynamic aeroelasticity. Alternative approaches are proposed by Quero et al. (2019) who employed tangential interpolation to construct generalized aeroelastic state space

* Corresponding author.
E-mail address: douglas.bueno@unesp.br (D.D. Bueno).

https://doi.org/10.1016/j.jfluidstructs.2021.103294
0889-9746/

models based on transfer functions. Lucia et al. (2005) used proper orthogonal decomposition and the Volterra theory to obtain state space models from a set of impulse responses that were processed using the Eigensystem Realization Algorithm. Smith et al. (2004) presented that linear and nonlinear curve fit techniques can be used to obtain aeroelastic state space models by matching the frequency responses of flexible aircraft. Marques and Azevedo (2008) investigated the z-Transform to obtain discrete state space models focused on stability analysis. Herdman and Turi (1991) noted that finite Hilbert transforms can be used to rewritten the airfoil equations through integral-based formulae. The approach provides a state space model suitable for control design.

Although different strategies have been investigated to obtain state space aeroelastic system representations, for the purpose of constructing a state space linear model, there is an alternative strategy from the classical linear algebra, as discussed in this article. Typically the methods used to approximate unsteady aerodynamics in the time domain consider constant coefficients proportional to the displacement, velocity and acceleration vectors. These coefficients are square matrices with dimensions equal to the number of the system's degrees of freedom. If the method also considers rational functions, additional constant coefficients are included proportional to the lag state vectors. On the other hand, Marqui et al. (2017) introduced an approach without considering the lag terms, and an accurate approximation is obtained because the problem is solved in two steps. In the first step, the Laguerre polynomial-based method computes constant coefficients used to write a polynomial series. The series is used later to compute the constant coefficients to write the aerodynamics proportional to the system's displacements, velocities and accelerations.

The results of Marqui et al. (2017) implicitly suggest that lag terms are added in those previous methods to compensate for the limitation of a one-step-based solution through the use of aerodynamic mass, stiffness and damping characteristics. Based on this idea, this article introduces a matrix dynamic model that is not dependent on the reduced frequency. It can be used to write the state space representation in the time domain through coupling of only aerodynamic stiffness and damping matrices. Instead of initially writing the aerodynamics in the frequency domain, the approach is focused on constructing the aeroelastic state space model directly. To obtain this representation, the classical iterative aeroelastic eigenvalue problem is solved using the *pk* method (Hassig, 1971). This is employed to construct a time domain aeroelastic model using a classical result from the linear algebra. The results show that this approach is a simple and efficient strategy to construct a state space representation for aeroelastic analysis in the time domain.

1. Methodology

Consider a second order aeroelastic model described through the mass matrix $\mathbf{M}$, the stiffness and damping structural matrices $\mathbf{K}$ and $\mathbf{B}$, respectively; and the unsteady aerodynamic matrix $\mathbf{Q}(k)$ defined for each reduced frequency k, such that

$$\mathbf{M}\ddot{\mathbf{u}}(t) + \mathbf{B}\dot{\mathbf{u}}(t) + \mathbf{K}\mathbf{u}(t) = q\mathbf{Q}(k)\mathbf{u}(\omega) \tag{1}$$

where $q = \frac{1}{2}\rho V^2$ is the dynamic pressure, ρ is the air density, V is the airspeed, $\mathbf{u}$ is the $n \times 1$ displacement vector, n is the number of degrees of freedom used to describe the system, t is the time and ω is the angular frequency. The reduced frequency is given by $k = \omega b/V$, ω is the angular frequency, and b is a characteristic length — commonly the aerodynamic semi-chord. Note that flap mechanisms may not need to be included in the model, as reported by Karpel (1981) and others.

2. State space model in the frequency domain

The aeroelastic state space representation can be obtained by considering a rearrangement of two system of equations. The first one is $\dot{\mathbf{u}} = \dot{\mathbf{u}}$, and although it is an obvious statement, it is helpful to understand the mathematical procedure. The second system of equations is obtained by pre-multiplying Eq. (1) by $\mathbf{M}^{-1}$, and isolating its second derivative $\ddot{\mathbf{u}}$. Note at this point that the matrix of structural mass $\mathbf{M}$ is typically a positive definite matrix. Considering that for this system of $2n$ equations all terms are expressed in the frequency domain, and defining conveniently $j\omega\mathbf{x}(\omega) = [j\omega\mathbf{u}(\omega) \ -\omega^2\mathbf{u}(\omega)]^T$, the classical frequency domain state space equation is achieved as follows

$$j\omega\mathbf{x}(\omega) = \mathbf{A}_k\mathbf{x}(\omega) \tag{2}$$

where the $\mathbf{A}_k$ dependent aeroelastic dynamic matrix is given by

$$\mathbf{A}_k = \begin{bmatrix} \mathbf{0}_{n\times n} & \mathbf{I}_n \\ -\mathbf{M}^{-1}(\mathbf{K} - q\mathbf{Q}_R) & -\mathbf{M}^{-1}\left(\mathbf{B} - \dfrac{q}{V}b\dfrac{\mathbf{Q}_I}{k}\right) \end{bmatrix} \tag{3}$$

Note that $\mathbf{A}_k$ corresponds to the matrix commonly used for flutter analysis using the method *pk* (Hassig, 1971), and the subscript k is used to indicate that the dynamic matrix depends on the reduced frequency k. Also, note that $\mathbf{A}_k \in \mathbb{R}^{2n\times 2n}$, $\mathbf{0}_{n\times n}$ is a $n \times n$ matrix of zeros, and $\mathbf{I}_n$ is an identity matrix. Eq. (2) does not readily admit to applying an inverse transform to be written in the time domain due to the unsteady aerodynamics dependence on k, as discussed in the literature.

3. State space model in the time domain

The aeroelastic ith mode $\psi_i \in \mathbb{C}^{n\times 1}$ is a subvector of the ith eigenvector $\Psi_i \in \mathbb{C}^{2n\times 1}$ extracted from matrix $\mathbf{A}_k$ *for each flight condition* (ρ, V), such that $\Psi_i = [\psi_i \;\; \lambda_i\psi_i]^T$. The eigenvectors are obtained in conjugate pairs, and the $2n \times 2n$ complex matrix of eigenvectors is given by $\mathbf{\Psi} = \begin{bmatrix}\Psi_1 & \Psi_1^* & \dots & \Psi_n & \Psi_n^*\end{bmatrix}$, where the superscript $*$ indicates the conjugate. The n pairs $(\lambda_i, \; \Psi_i)$ can be obtained by solving the classical aeroelastic iterative eigenvalue problem $[\mathbf{A}_k - \lambda_i\mathbf{I}_{2n}]\,\Psi_i = \mathbf{0}$, $i = 1, \dots, 2n$ defined from the first equation in Eq. (2) by setting $j\omega = \lambda_i$ and $\mathbf{x}(\omega) = \Psi_i$.

3.1. Dynamic matrix construction

Assuming there is an aerodynamic force vector $\mathbf{F}_a(t) = \mathbf{Q}_0\mathbf{u}(t) + \mathbf{Q}_1\dot{\mathbf{u}}(t)$ that is able to introduce the effects of $q\mathbf{Q}(k)\mathbf{u}(s)$ in the time domain *for each particular dynamic pressure*, then the second order aeroelastic equation (Eq. (1)) is rewritten through the aeroelastic stiffness matrix $\mathbf{K}_a = \mathbf{K} - \mathbf{Q_0}$ and damping $\mathbf{B}_a = \mathbf{B} - \mathbf{Q}_1$, and eliminating the right hand side term. This assumption allows one to write the constant dynamic matrix $\mathbf{A}$ as follows

$$\mathbf{A} = \begin{bmatrix} \mathbf{0}_{n\times n} & \mathbf{I}_n \\ -\mathbf{M}^{-1}\mathbf{K}_a & -\mathbf{M}^{-1}\mathbf{B}_a \end{bmatrix} \tag{4}$$

Note that the assumption described above is conceptually equivalent to assuming that $q\mathbf{Q}(k)$ can be described by $\mathbf{Q}_0 + j\omega\mathbf{Q}_1$. However, note that if aerodynamic approximation is performed, lag terms are included to achieve accurate results (Roger, 1977; Karpel, 1981). In addition, the Laguerre-polynomial-based method shows that a matrix proportional to the accelerations is also necessary to approximate the aerodynamics (Marqui et al., 2017). On the other hand, note that instead of computing the matrices $\mathbf{Q}_0$ and $\mathbf{Q}_1$, it is possible construct the dynamic matrix directly. This is possible using the eigenvectors and eigenvalues, as known from the classical linear algebra. The eigensolution can be easily obtained in the frequency domain by solving the iterative problem formulated through the *pk* method.

Let $\mathbf{\Lambda} = diag(\lambda_i, \; \lambda_i^*, \; \dots, \; \lambda_n, \; \lambda_n^*)$ be the matrix of eigenvalues extracted from the matrix $\mathbf{A}_k$. Then, the $2n$ equations (or, equivalently, n pairs conjugate equations) previously written as

$$\begin{cases} \mathbf{A}_k\Psi_1 = \lambda_1\Psi_1 \\ \mathbf{A}_k\Psi_1^* = \lambda_1^*\Psi_1^* \\ \quad\vdots \\ \mathbf{A}_k\Psi_n = \lambda_1\Psi_n \\ \mathbf{A}_k\Psi_n^* = \lambda_1\Psi_n^* \end{cases} \tag{5}$$

can be rearranged in matrix form, such that

$$\mathbf{A}\begin{bmatrix}\Psi_1 & \Psi_1^* & \dots & \Psi_n & \Psi_n^*\end{bmatrix} = \begin{bmatrix}\Psi_1 & \Psi_1^* & \dots & \Psi_n & \Psi_n^*\end{bmatrix}\mathbf{\Lambda} \tag{6}$$

This strategy can be employed because it is desired to construct a constant matrix $\mathbf{A}$ containing the same aeroelastic frequencies, damping ratios and modes as obtained from $\mathbf{A}_k$.

Denoting $\mathbf{\Psi}^{-1} = \tilde{\mathbf{\Psi}}$ to simplify the notation, and post-multiplying Eq. (6) by $\tilde{\mathbf{\Psi}}$, the matrix $\mathbf{\Psi\Lambda\tilde{\Psi}}$ can be conveniently separated into real and imaginary parts. In practice, this means that $\mathbf{A} = \mathbf{A}^R + j\mathbf{A}^I$, where the superscripts R and I indicate the real and imaginary parts, respectively, such that

$$\begin{aligned} \mathbf{A}^R &= \mathbf{\Psi}^R\mathbf{\Lambda}^R\tilde{\mathbf{\Psi}}^R - \mathbf{\Psi}^I\mathbf{\Lambda}^R\tilde{\mathbf{\Psi}}^I - \mathbf{\Psi}^I\mathbf{\Lambda}^I\tilde{\mathbf{\Psi}}^R - \mathbf{\Psi}^R\mathbf{\Lambda}^I\tilde{\mathbf{\Psi}}^I \\ \mathbf{A}^I &= \mathbf{\Psi}^I\mathbf{\Lambda}^R\tilde{\mathbf{\Psi}}^R + \mathbf{\Psi}^R\mathbf{\Lambda}^R\tilde{\mathbf{\Psi}}^I + \mathbf{\Psi}^R\mathbf{\Lambda}^I\tilde{\mathbf{\Psi}}^R - \mathbf{\Psi}^I\mathbf{\Lambda}^I\tilde{\mathbf{\Psi}}^I \end{aligned} \tag{7}$$

where $\mathbf{A}^I \equiv \mathbf{0}_{2n\times 2n}$ is consistent with the matrix $\mathbf{A}_k$ which is a $2n \times 2n$ matrix of real numbers.[1] However, whereas $\mathbf{A}_k$ depends on the frequency,[2] the matrices in Eq. (7) do not. Based on these results, the dynamic matrix can be defined by a compact notation and is given by

$$\mathbf{A} = \Re\left(\mathbf{\Psi\Lambda\Psi}^{-1}\right) \tag{8}$$

where $\Re(\;)$ indicates the real part of this matrix product.

It is important to highlight that the $\mathbf{A}^I$ obtained computationally in numerical solutions typically exhibits very small magnitudes that can be neglected in practical problems. These values can be evaluated by considering a simple normalized matrix norm-2, defined as follows

$$\varepsilon_I = \frac{\|\mathbf{A}^I\|_2}{\|\mathbf{A}^R\|_2} \tag{9}$$

where $\|\mathbf{A}^{(\,)}\|_2 = \sigma\left(\mathbf{A}^{(\,)}\right)$ is the largest singular value of $\mathbf{A}^{(\,)}$.

[1] Computationally $\mathbf{A}^I$ can exhibit small numbers which can be neglected.

[2] Note it explicitly depends on the reduced frequency k.

3.2. Dynamic matrix sensitivity to the flight condition

The dynamic matrix defined by Eq. (8) is computed *for each flight condition*, as previously mentioned. Thus, it is as sensitive to the flight condition as the aeroelastic modes ψ_i, frequencies $\omega_i = \Im(\lambda_i)$ and decay ratios $\gamma_i = \Re(\lambda_i)$ are. The ith aeroelastic mode ψ_i is obtained from the n first rows of each ith eigenvector Ψ_i, neglecting the conjugates $(\lambda_i^*,\ \Psi_i^*)$. Decay ratios are more sensitive to the flight conditions than frequencies, although both of them change in the operational flight envelope. Typically decay ratios change more substantially — vide classical V-g-f diagrams (Chipman and Shyprykevich, 1974; De Marqui Junior et al., 2007). On the other hand, two different flight conditions can result in similar aeroelastic mode shapes. This feature is well known, and can be used to track modes during flight flutter tests (Desforges et al., 1996).

Consider two different flight conditions $\mathbb{F}_1 := (M_{a(1)}, \rho_1, V_1)$ and $\mathbb{F}_2 := (M_{a(2)}, \rho_2, V_2)$, where $M_{a(\,)}$ is the Mach number, and their respective eigenpairs $\left(\mathbf{\Lambda}_{\mathbb{F}_1},\ \mathbf{\Psi}_{\mathbb{F}_1}\right)$ and $\left(\mathbf{\Lambda}_{\mathbb{F}_2},\ \mathbf{\Psi}_{\mathbb{F}_2}\right)$. The similarity measure between two sets of mode shapes can easily obtained by computing the Modal Assurance Criterion MAC, as follows (Allemang, 2003; Pastor et al., 2012)

$$\mathrm{MAC}_{xy} = \frac{\left|\psi_{\mathbb{F}_1(x)}^T\ \psi_{\mathbb{F}_2(y)}^*\right|^2}{\left(\psi_{\mathbb{F}_1(x)}^T\psi_{\mathbb{F}_1(x)}^*\right)\left(\psi_{\mathbb{F}_2(y)}^T\psi_{\mathbb{F}_2(y)}^*\right)} \tag{10}$$

where $\left[\psi_{\mathbb{F}_1(1)}\ \ldots\ \psi_{\mathbb{F}_1(x)}\ \ldots\ \psi_{\mathbb{F}_1(n)}\right]$ and $\left[\psi_{\mathbb{F}_2(1)}\ \ldots\ \psi_{\mathbb{F}_2(y)}\ \ldots\ \psi_{\mathbb{F}_2(n)}\right]$ respectively obtained from $\mathbf{\Psi}_{\mathbb{F}_1}$ and $\mathbf{\Psi}_{\mathbb{F}_2}$, $x, y = 1, \ldots, n$. The superscripts T and $*$ indicate respectively the transpose and conjugate vectors. Assuming a high value of MAC_{xx} for the n modes, i.e., the xth mode for $\mathbb{F}_1$ is similar to the xth mode for $\mathbb{F}_2$, the dynamic matrix for the second flight condition can be written as

$$\mathbf{A}_{\mathbb{F}_2} = \Re\left(\mathbf{\Psi}_{\mathbb{F}_1}\mathbf{\Lambda}_{\mathbb{F}_2}\mathbf{\Psi}_{\mathbb{F}_1}^{-1}\right) \tag{11}$$

Note that these two modal shapes are highly similar (i.e., correlated and almost identical) if $0.9 \leq \mathrm{MAC}_{xx} \leq 1$. Also, note that $\mathbf{A}_{\mathbb{F}_2}$ describes the flight condition $\mathbb{F}_2$, although it uses the aeroelastic modal matrix computed for $\mathbb{F}_1$. Eq. (11) shows a strategy which allows one, for example, to reduce the requirement of computational data storage because the same set of eigenvectors can construct the dynamic matrix for more than one flight condition. This possibility is valuable for industrial applications, in which many different dynamic models are used to describe different mass configurations, to perform parametric analysis, etc.

3.3. System representation

Using these previous results, the state space frequency response function (FRF) is given by $\mathbf{H}_{ss}(\omega) = \mathbf{C}\left[j\omega\mathbf{I} - \mathbf{A}_k\right]^{-1}\mathbf{B}_c$ as defined in the literature (Ogata, 1990). Note that the matrix $\mathbf{A}$ (Eq. (8)) can alternatively be used instead of $\mathbf{A}_k$. On the other hand, only $\mathbf{A}$ can directly be used to write the time domain representation shown below

$$\begin{aligned}\dot{\mathbf{x}}(t) &= \mathbf{A}\mathbf{x}(t) + \mathbf{B}_c\mathbf{u}_c(t)\\ \mathbf{y}(t) &= \mathbf{C}\mathbf{x}(t)\end{aligned} \tag{12}$$

Appendix B shows how the input matrix $\mathbf{B}_c$ and the output matrix $\mathbf{C}$ can be obtained.

3.3.1. Generalized coordinate system

If the aeroelastic system is described in generalized coordinates, typically considered are the structural undamped modes ϕ_i, such that $\left(\mathbf{M}^{-1}\mathbf{K} - \lambda_i\mathbf{I}_n\right)\phi_i = \mathbf{0}, i = 1, \ldots, n$. The physical displacement vector is written as $\mathbf{u} = [\phi_1\ \ldots.\ \phi_n]\,\mathbf{u}_\phi$, where $\mathbf{u}_\phi$ is the vector of modal displacements and $\mathbf{\Phi} = [\phi_1\ \ldots.\ \phi_n]$ is the modal matrix.[3]

Let $\tilde{\mathbf{\Phi}}$ be the $2n \times 2n$ matrix such that

$$\tilde{\mathbf{\Phi}} = \begin{bmatrix}\mathbf{\Phi} & \mathbf{0}_{n\times n}\\ \mathbf{0}_{n\times n} & \mathbf{\Phi}\end{bmatrix} \tag{13}$$

the state space system representation in generalized coordinates is obtained by considering $\mathbf{x} = \tilde{\mathbf{\Phi}}\mathbf{x}_\phi$ and pre-multiplying both sides of Eq. (12) by $\tilde{\mathbf{\Phi}}^{-1}$. If the modal matrix is such that $\det(\tilde{\mathbf{\Phi}}) = \pm 1$, its inverse can be replaced by $\tilde{\mathbf{\Phi}}^T$. For this coordinate system, the dynamic matrix is given by $\tilde{\mathbf{\Phi}}^{-1}\mathbf{A}_{\mathbb{F}_2}\tilde{\mathbf{\Phi}} = \mathbf{A}_{\mathbb{F}_2}^{\phi}$, and each ith eigenvector Ψ_i is $\{\psi_i^\phi\ \ \lambda_i\psi_i^\phi\}^T$. The ith aeroelastic mode ψ_i is given by

$$\psi_i = \mathbf{\Phi}\psi_i^\phi \tag{14}$$

In practical problems, the generalized coordinates are used to truncate the system representation. For these cases, $\mathbf{\Phi}$ is $n \times m$, for $m \ll n$, and the dynamic matrix becomes $2m \times 2m$. The displacement of the ith degree of freedom is given by $u_i = \sum_{j=1}^{m}\phi_{ij}u_{\phi(j)} + \epsilon_i$, where ϵ_i is a truncation error. See Gawronski (2004) for a detailed description of this type of model reduction strategy.

[3] Note that it is the structural modal matrix, i.e., it does not correspond to the aeroelastic modes.

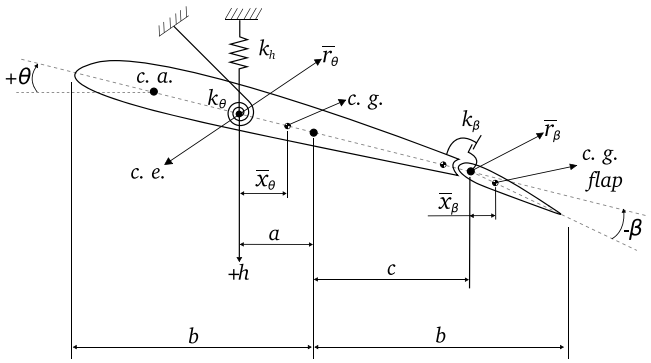

Fig. 1. Typical section 2D airfoil.

Table 1
Geometric properties for the 3 DOF airfoil.

$a = -0.40$	$c = 0.60$	$x_\theta = 0.20$
$x_\beta = 0.0125$	$r_\theta = 0.22$	$r_\beta = 0.035$

4. Results and discussions

To demonstrate the proposed approach for constructing the dynamic matrix for a state space system representation, a three degrees of freedom airfoil is considered (Theodorsen, 1935). The system is defined by the modes of plunge h, pitch θ, and control surface rotation β. The mass per span is equal to $M = 3$ [kg/m], the aerodynamic semi-chord $b = 0.3$ [m], the air density $\rho = 1.225$ [kg/m^3]. The uncoupled plunge structural frequency is assumed equal to 6 [Hz] and, similarly, the pitch and the control surface rotation modes respectively equal to 11 and 18 [Hz]. Table 1 shows the geometrical properties used to define the aerofoil dynamics (see Fig. 1).

Figs. 2b and 2a compare respectively the V-f and V-g diagrams obtained using the pk method (i.e., from $\mathbf{A}_k$) and from the constant matrix $\mathbf{A}$. The pk solution indicates that the third mode becomes unstable to define the flutter at $V_f = 25.5$ m/s with frequency $f_f = 16.7$ Hz. Because Eq. (8) is an exact solution, there are only small numerical errors, and for this example they are smaller than 10^{-13} for both aeroelastic frequencies f and damping ratios g. Also, the maximum ε_I observed for this case is 8.1×10^{-15}, using a conventional double precision personal computer with a 64-bit Linux operating system.

The FRFs for coincident input and output are shown in Figs. 3a through 3c respectively for the plunge, pitch and control surface rotation degrees of freedom. The differences between the results obtained using the matrices $\mathbf{A}_k$ and $\mathbf{A}$ are higher for the pitch and control surface rotation FRFs. See Appendix A for details on the relative errors. They exist because the matrix $\mathbf{A}$ is constructed considering the system characteristics only for n frequencies, i.e., the number of degrees of freedom (or the number of modes if a truncated representation in generalized coordinates is employed), whereas $\mathbf{A}_k$ is computed for each particular frequency. The results are computed by using $\mathbf{B}_0 = \mathbf{I}_3$ and $\mathbf{C} = [\mathbf{I}_3 \;\; \mathbf{0}_{3\times 3}]$. The results for the other FRFs are similar to these ones. In addition, because the matrix $\mathbf{A}$ describes the system's stability accurately (see V-g-f diagrams), it can be employed to perform analysis in the time domain. Fig. 4 shows the system's response for $V = 1.02V_f$ considering an initial condition $h(0) = -0.004$ m, and it is possible to observe that the third mode is unstable, as predicted in the frequency domain.

MAC is computed to evaluate how sensitive the dynamic matrix is to the flight condition. Fig. 5 shows the values for the three modes. It is considered $\mathbb{F}_1 := \left(\rho, \sim 0.8V_f\right)$, i.e., the fixed matrix of eigenvectors Ψ_1, and $\mathbb{F}_2$ is represented by $\mathbf{\Lambda}_i$ for each ith flight condition (in this case, a fixed ρ for a range of airspeeds). It is verified that there are higher values of MAC for the first (plunge) and third modes (control surface rotation). However, the minimum value of MAC for the second mode is higher than 0.86. The V-g-f diagram is accurately constructed from the eigenvalues of $\mathbf{A}_{\mathbb{F}_2}$ in comparison with the pk method. Numerical difference between the results from $\mathbf{A}$ (Eq. (8)) and $\mathbf{A}_{\mathbb{F}_2}$ (Eq. (11)) is around 10^{-13} for this case.

4.1. Agard 445.6 wing

The approach proposed herein is also evaluated for the AGARD 445.6 wing described in the generalized coordinate system considering twenty modes. The AGARD 445.6 wing is represented by using the Finite Element method for describing the structural characteristics and the Doublet Lattice method for aerodynamics (Albano and Rodden, 1969). For this model the thickness distribution is governed by the airfoil shape. The material properties used are $E_1 = 3.1511$, $E_2 = 0.4162$ GPa, $\nu = 0.31$, $G = 0.4392$ GPa and $\rho_{\text{mat}} = 381.98$ kg/m^3, where E_1 and E_2 are the moduli of elasticity in

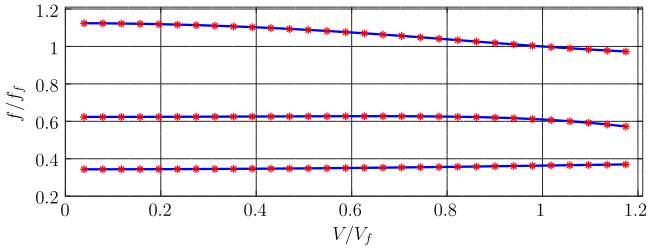

(a) V-g

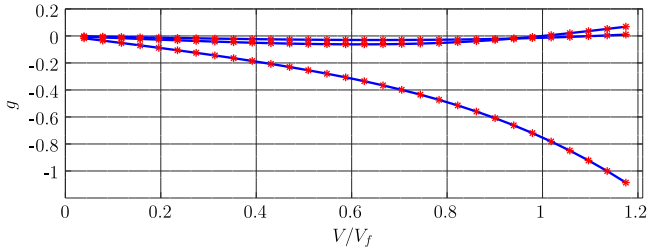

(b) V-f

Fig. 2. (a) V-f and (b) V-g diagrams obtained using the *pk* method (solid line) and the eigenvalues of **A**.

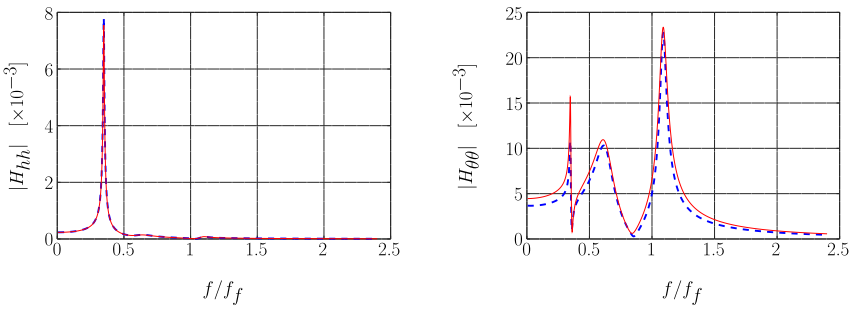

(a) (b)

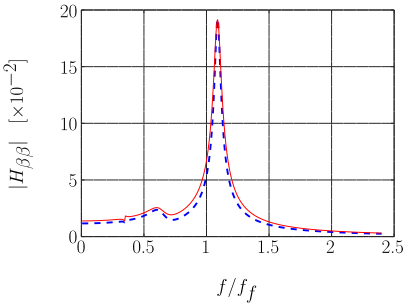

(c)

Fig. 3. Aeroelastic FRF for the (a) plunge, (b) pitch and (c) control surface rotation degrees of freedom using: $\mathbf{A}_k$ (dashed line) and **A** (solid thin line).

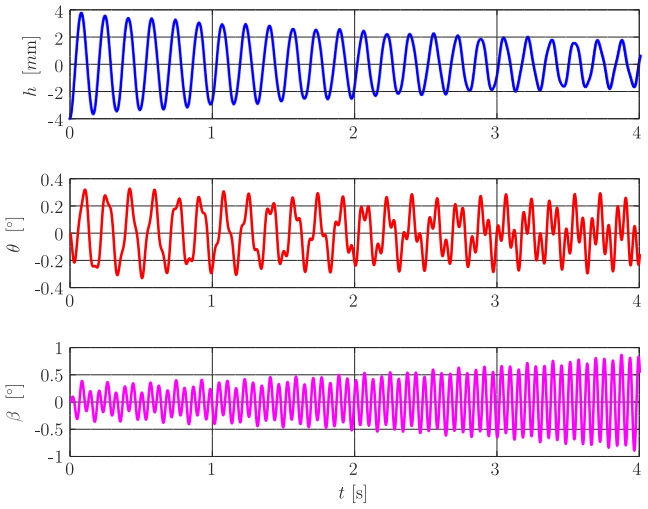

Fig. 4. Aeroelastic time responses for an unstable condition computed using the **A**.

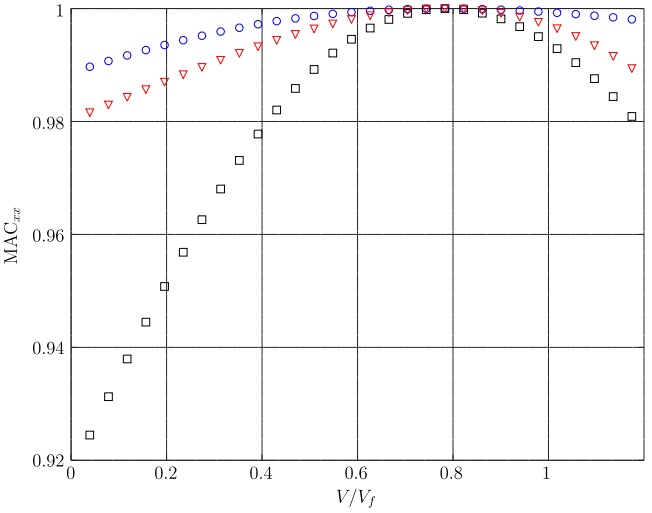

Fig. 5. MAC computed for the typical section: first mode (blue circle), second mode (black square) and third mode (red triangle).

Table 2
Reduced frequencies for the case study AGARD wing 445.6.

10^{-3}	2.10^{-3}	5.10^{-3}	10^{-2}
0.05	0.1	0.2	0.3
0.5	0.6	0.8	1.0
1.5	2.0	3.0	4.0

the longitudinal and lateral directions, ν is Poisson's ratio, G is the shear modulus in each plane and ρ is the wing density. Table 2 shows the reduced frequencies k used to compute the aerodynamic matrices. See complementary details in Bueno et al. (2013) and references cited therein.

Figs. 6a and 6b show respectively the V-f and V-g diagrams obtained using the pk method, and by extracting the eigenvalues of **A**. Although these figures only show the first four modes, the differences among aeroelastic frequencies and damping ratios are smaller than 10^{-11}, and it is verified that $\varepsilon_I < 8.7 \times 10^{-14}$. The results are shown normalized by the velocity and frequency of flutter ($V_f = 113$ m/s and $f_f = 13.3$ Hz), and they demonstrate that the approach can easily be applied to multiple degrees of freedom systems described by generalized coordinates.

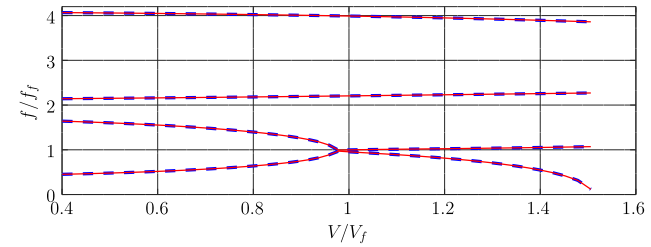

(a) V-f

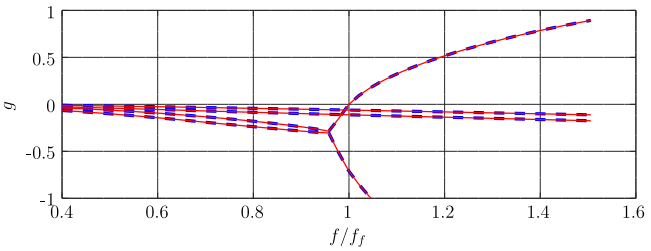

(b) V-g

Fig. 6. V-f and V-g diagrams obtained using the *pk* method (solid line) and the eigenvalues of **A** (AGARD 445.6 wing).

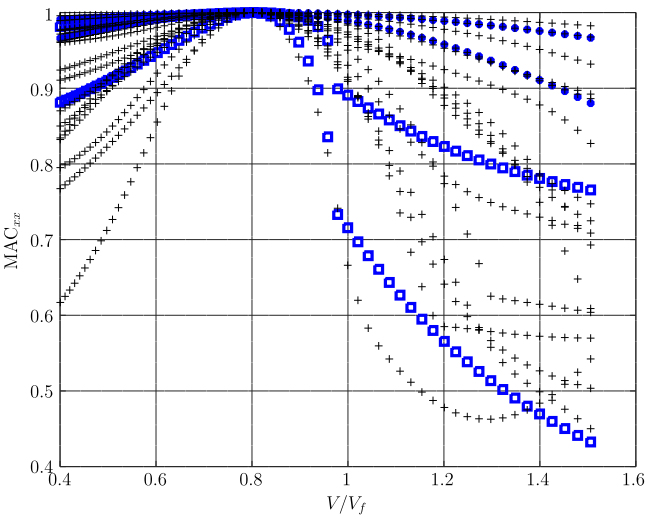

Fig. 7. MAC computed for the AGARD 445.6 wing: first two modes (blue square), third and fourth modes (blue dots), other modes (black +).

Fig. 7 shows the values of MAC for twenty modes of the AGARD wing. It is considered $\mathbf{\Psi}_{\mathbb{F}_1}$ for[4] $V_{ea} = 0.8V_{ea(f)}$ at Mach number 0.50. High values are verified for the first four modes for $V < V_f$ and low similarity is observed for modes with frequencies $f/f_f > 5$. The V-g-f diagram for this system can be accurately constructed using the eigenvalues of $\mathbf{A}_{\mathbb{F}_2}$. On the other hand, although the stability characteristics are preserved in the frequency and time domains (see Fig. 8), amplitudes of time domain responses present differences as shown in Fig. 9 for a flight condition $V_{ea} = 0.63V_{ea(f)}$. In the case shown in Fig. 9, the relative energy of the signals computed using $\mathbf{A}_{\mathbb{F}_2}$ are respectively equal to 55% and 367% in relation to **A** (see Appendix A.1 for details). Due to the truncation errors associated with the system representation in generalized coordinates, the dynamic matrix becomes more sensitive to the flight condition variation. For these cases, it is convenient to use the matrix **A** instead of $\mathbf{A}_{\mathbb{F}_2}$ (note that, in practice, it is $\mathbf{A}^{\phi}_{\mathbb{F}_2}$) for applications involving accurate amplitude estimation, such as gust response analysis.

[4] V_{ea} is the as equivalent airspeed $V_{ea} = V\sqrt{\rho/\rho_0}$, where $\rho = 1.225$ kg/m^3.

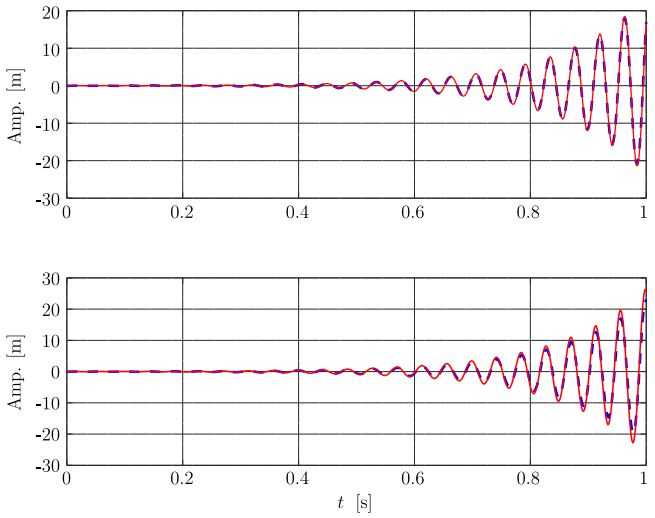

Fig. 8. Aeroelastic time responses for AGARD 445.6 wing computed using **A** (dashed line) and $\mathbf{A}_{\mathbb{F}_2}$ (thin solid line) for an unstable flight condition in two different degrees of freedom (upper and lower pictures).

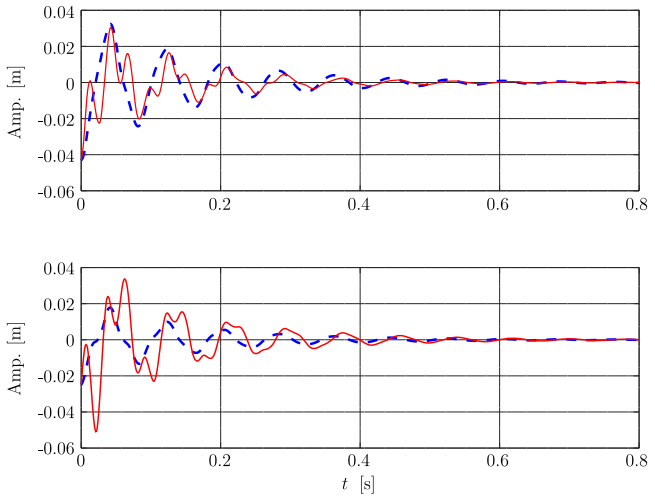

Fig. 9. Aeroelastic time responses for AGARD 445.6 wing computed using **A** (dashed line) and $\mathbf{A}_{\mathbb{F}_2}$ (thin solid line) for a stable flight condition in two different degrees of freedom (upper and lower pictures).

5. Final remarks

This article has presented a dynamic matrix that can easily be constructed for aeroelastic analysis in the time domain using the eigensolution from the *pk* method. The approach employs a classical result from linear algebra, demonstrating that is not necessary to write unsteady aerodynamics in the time domain before constructing a state space representation for an aeroelastic system. The approach is directly valid for linear and piecewise linear models, but further investigations are needed to evaluate its applicability for nonlinear models. Using this time domain representation it is possible to design controllers based on the state space realization, such as the Linear Quadratic (LQ) Regulator, LQ Gaussian, and others, for active flutter control and gust load alleviation.

In comparison with the use of rational function (RFA) techniques to obtain the state space model, there are two main advantages in using the approach introduced in this article: (*i*) the dynamic matrix dimension is $2n \times 2n$, instead of $n(2+n_{lag}) \times n(2+n_{lag})$, where n_{lag} is the number of lag states. This is helpful mainly when considering a large number of modes (in the generalized coordinates) or degrees of freedom (when using the physical coordinate system); (*ii*) the new method does not require aerodynamic approximations, as required by RFA techniques.

The results show that if the aeroelastic system is described in generalized coordinates the state space dynamic matrix can also be obtained. The illustrative example using the AGARD 445.6 wing demonstrates that aeroelastic dynamic stability characteristics are preserved for multiple degrees of freedom systems in both the frequency and time domains.

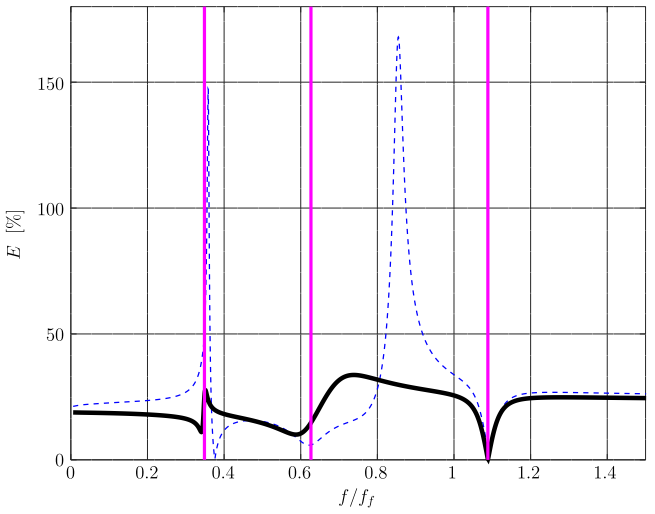

Fig. A.10. Relative error between the FRF obtained using the matrices $\mathbf{A}_k$ and $\mathbf{A}$: pitch (dashed-line) and control surface rotation (solid lined). The vertical lines indicates the frequencies of the aeroelastic modes.

The present work also discussed the dynamic matrix sensitivity to the flight condition. It was demonstrated that a unique set of eigenvectors from *pk* method can be used to construct the aeroelastic dynamic matrix for different flight conditions. However, the specific set of eigenvalues must be used because aeroelastic frequencies and decay ratios are more sensitive to the flight condition than the aeroelastic modes. In particular for a system described in generalized coordinates, truncation errors may affect the response amplitudes if a different set of eigenvectors is used to construct the aeroelastic dynamic matrix. On the other hand, if generalized coordinates are considered without truncation, i.e., considering all structural undamped modes, amplitudes can be computed accurately. Although omitted, for the sake of brevity, this result was also verified for the typical section considering its three modes.

CRediT authorship contribution statement

Douglas D. Bueno: Conceptualization, Formal analysis, Funding acquisition, Methodology, Software, Writing - original draft, Writing - review & editing. **Earl H. Dowell:** Supervision, Writing - original draft, Writing - review & editing.

Declaration of competing interest

The authors declare that they have no known competing financial interests or personal relationships that could have appeared to influence the work reported in this paper.

Acknowledgment

The first author thanks the São Paulo Research Foundation (FAPESP), Brazil, Grant no. 18/25194-6 for funding this research.

Appendix A. Relative errors in the FRFs

The relative error E can be used to compare the two FRFs obtained using the matrices $\mathbf{A}_k$ and $\mathbf{A}$. The error is computed for the pitch ($H_{\theta\theta}$) and the control surface rotaion ($H_{\beta\beta}$), for which the FRFs are shown in Figs. 3b and 3c, respectively. The error is defined as follows:

$$E = 100\frac{\left|H_{(\,)}(\mathbf{A}_k) - H_{(\,)}(\mathbf{A})\right|}{|H_{(\,)}(\mathbf{A}_k)|} \tag{A.1}$$

where $H_{(\,)}(\mathbf{A}_k)$ denotes the FRF computed using matrix $\mathbf{A}_k$ and $H_{(\,)}(\mathbf{A})$ using $\mathbf{A}$. It is noted that smaller relative errors are obtained for frequencies near the modal frequencies (see vertical lines as references). On the other hand, higher relative errors are obtained for frequencies in which aeroelastic antiresonances are observed. However, these have a small influence on the system response. (see Fig. A.10).

A.1. Signal energy

The relative energy E_s computed for the signals shown in Fig. 9 is computed by

$$E_s = \frac{\sum_{i=1}^{N} \left(y_i - y_i^{\mathbb{F}_2}\right)^2}{\sum_{i=1}^{N} y_i^2} \tag{A.2}$$

where i indicates the ith time instant, y_i is signal computed using $\mathbf{A}$ and $y_i^{\mathbb{F}_2}$ is signal computed using $\mathbf{A}_{\mathbb{F}_2}$.

Appendix B. Multiple input and multiple output system

The complete state space equation is obtained if an additional $r \leq n$ external inputs $\mathbf{u}_c = \{u_{c(1)}, \ ..., \ u_{c(r)}\}^T$ are considered (generically describing gust loads or control forces, for example). Assuming they act in any r of n degrees of freedom, the $n \times 1$ vector $\mathbf{B}_0\mathbf{u}_c$ is considered on the right hand side of Eq. (1), where $\mathbf{B}_0$ is a $n \times r$ matrix such that its zth column ($z = 1, \ldots, r$) is $[0 \ \ \ldots \ \ 0 \ \ 1|_i \ \ 0 \ \ \ldots \ \ 0]^T$, i.e., $b_{iz} = 1$ if the zth input acts on the i degree of freedom. In particular, the $r = n$ and the vector $\mathbf{u}_c$ is such that each ith input is its ith element (i.e., it acts on each respective ith dof), $\mathbf{B}_0$ is an identity matrix if there is input in all degrees of freedom. Using this result, the input matrix $\mathbf{B}_c = [\mathbf{0}_{n\times r} \ \ \mathbf{M}^{-1}\mathbf{B}_0]^T$ can be considered in the state space equation. Note that the input matrix $\mathbf{B}_c$ does not depends on the aerodynamics.

A general state space representation also admits $s \leq n$ outputs. It is necessary to consider the equation $\mathbf{y} = \mathbf{C}\mathbf{x}$, where $\mathbf{y}$ is the vector of outputs and $\mathbf{C}$ is the $s \times 2n$ output matrix. Gawronski (2004) employs a convenient notation separating this matrix such that $\mathbf{C} = [\mathbf{C}_d \ \ \mathbf{C}_v]$, where the subscripts respectively indicate outputs of displacements and velocities, respectively. In particular, the outputs corresponding to the states, $\mathbf{C}_d$ and $\mathbf{C}_v$ are constructed similarly to the matrix $\mathbf{B}_0$; otherwise, they are defined conveniently to combine and/or convert the states properly.

References

Abel, I., 1979. An Analytical Technique for Predicting the Characteristics of a Flexible wing Equipped with an Active Flutter-Suppression System and Comparison with Wind-Tunnel Data. TP 1367, National Aeronautical and Space Administration - NASA.

Albano, E., Rodden, W.P., 1969. A doublet-lattice method for calculating lift distributions on oscillating surfaces in subsonic flows. AIAA J. 7 (2), 279–285.

Allemang, A.J., 2003. The modal assurance criterion (MAC): Twenty years of use and abuse. Sound Vib. 14–21.

Bernal, D., 2008. In: O.S., B., D., W. (Eds.), Modern Testing Techniques for Structural Systems. In: CISM International Centre for Mechanical Sciences, vol. 502, Springer, Vienna, pp. 97–129. http://dx.doi.org/10.1007/978-3-211-09445-7_2.

Biskri, D., Botez, R.M., Stathopoulos, N., Therien, S., Rathe, A., Dickinson, M., 2006. New mixed method for unsteady aerodynamic force approximations for aeroservoelasticity studies. J. Aircr. 43 (5), 1538–1541.

Bueno, D.D., Goes, L.C.S., Gonçalvez, P.J.P., 2015. Flutter analysis including structural uncertainties. Meccanica 50, 2093–2101. http://dx.doi.org/10.1007/s11012-015-0138-8.

Bueno, D.D., Marqui, C.R., Goes, L.C.S., Gonçalves, P.J.P., 2013. The use of gramian matrices for aeroelastic stability analysis. Math. Probl. Eng. 2013, 941689. http://dx.doi.org/10.1155/2013/941689, 9 pgs.

Chipman, R.R., Shyprykevich, P., 1974. Analysis of Wing-Body Interaction Flutter for a Preliminary Space Shuttle Design. Contractor Report CR-2429, National Aeronautics and Space Administration (NASA), USA.

De Jesus-Mota, S., Beaulieu, M.N., Botez, R.M., 2009. Identification of a MIMO state space model of an F/A-18 aircraft using a subspace method. Aeronaut. J. 113 (1141).

De Marqui Junior, C., Rebolho, D.C., Belo, E.M., Marques, F.a.D., Tsunaki, R.H., 2007. Design of an experimental flutter mount system. J. Braz. Soc. Mech. Sci. Eng. 29, 246–252.

Desforges, M., Cooper, J.E., Wright, J.R., 1996. Mode tracking during flutter testing using the modal assurance criterion. Proc. Inst. Mech. Eng. G 210 (1), 27–37, arXiv:https://doi.org/10.1243/PIME_PROC_1996_210_342_02.

Dinu, A.D., Botez, R.M., Cotoi, I., 2005. Aerodynamic forces approximations using the Chebyshev method for closed-loop aeroservoelasticity studies. Canad. Aeronaut. Space J. 51 (4), 1–9.

Gawronski, W., 2004. Dynamics and Control of Structures: A Modal Approach. In: Mechanical Engineering Series, Springer New York.

Gennaretti, M., Mastroddi, F., 2004. Study of reduced-order models for gust-response analysis of flexible wings. J. Arcraft 41 (2).

Gennaretti, M., Muro, D., 2012. Multiblade reduced-order aerodynamics for state-space aeroelastic modeling of rotors. J. Aircr. 49 (2), 495–502. http://dx.doi.org/10.2514/1.C031422, arXiv:https://doi.org/10.2514/1.C031422.

Gori, R., Serafini, J., Molica Colella, M., Gennaretti, M., 2016. Assessment of a state-space aeroelastic rotor model for rotorcraft flight dynamics. CEAS Aeronaut. J. 7, 405–418. http://dx.doi.org/10.1007/s13272-016-0196-1.

Harmin, M.Y., Cooper, J.E., 2011. Aeroelastic behaviour of a wing including geometric nonlinearities. Aeronaut. J. 115 (1174).

Hassig, H.J., 1971. An approximate true damping solution of the flutter equation by determinant iteration. J. Aircr. 8 (11), 885–889.

Herdman, T.L., Turi, J., 1991. An application of finite Hilbert transforms in the derivation of a state space model of an aeroelastic system. J. Integral Equ. Appl. 3 (2), 271–287.

Jo, N.H., Seo, J.H., 2000. Input output linearization approach to state observer design for nonlinear system. IEEE Trans. Automat. Control 45 (12), 2388–2393. http://dx.doi.org/10.1109/9.895580.

Kalman, R., 1960. A new approach to linear filtering and prediction problems. Trans. ASME - J. Basic Eng. 82 (Series D), 35–45.

Karpel, M., 1981. Design for Active and Passive Flutter Suppression and Gust Alleviation. TR 3482, National Aeronautics and Space Administration - NASA.

Lucia, D.J., Beran, P.S., Silva, W.A., 2005. Aeroelastic system development using proper orthogonal decomposition and Volterra theory. J. Aircr. 42 (2), 509–518. http://dx.doi.org/10.2514/1.2176, arXiv:https://doi.org/10.2514/1.2176.

Marques, A.N., Azevedo, J.L.F., 2008. A z-transform discrete-time state-space formulation for aeroelastic stability analysis. J. Aircr. 45 (5), 1564–1578. http://dx.doi.org/10.2514/1.32561, arXiv:https://doi.org/10.2514/1.32561.

Marqui, C.R., Bueno, D.D., Goes, L.C., Gonçalves, P.J., 2017. A reduced order state space model for aeroelastic analysis in time domain. J. Fluids Struct. 69, 428–440. http://dx.doi.org/10.1016/j.jfluidstructs.2017.01.010, URL: http://www.sciencedirect.com/science/article/pii/S0889974616301815.

Mukhopadhyay, V., 1999. Transonic flutter suppression control law design, analysis and wind-tunnel results. In: International Forum on Aeroelasticity and Structural Dynamics - IFASD. Williamsburg, VA. p. 12.

Ogata, K., 1990. Modern Control Engineering, second ed. Prentice Hall PTR, Upper Saddle River, NJ, USA.

van Overschee, P., de Moor, L., 1996. Subspace Identification for Linear Systems: Theory, Implementation, Applications, Vol. 1. Kluwer Academic Publishers.

Pastor, M., Binda, M., Harcarik, T., 2012. Modal assurance criterion. Procedia Eng. 48, 543–548. http://dx.doi.org/10.1016/j.proeng.2012.09.551, URL: http://www.sciencedirect.com/science/article/pii/S1877705812046140; Modelling of Mechanical and Mechatronics Systems.

Quero, D., Vuillemin, P., Poussot-Vassal, C., 2019. A generalized state-space aeroservoelastic model based on tangential interpolation. Aerospace 6 (7), http://dx.doi.org/10.3390/aerospace6010009.

Roger, K., 1977. Airplane math modelling methods for active control design. In: AGARD Conference Proceeding, Vol. 9. pp. 4.1–4.11.

Roughen, K.M., Bendiksen, O.O., Baker, M.L., 2009. Development of generalized aeroservoelastic reduced order models. In: 50th AIAA/ASME/ASCE/AHS/ASC Structures, Structural Dynamics, and Materials Conference. AIAA 2009-2491, American Institute of Aeronautics and Astronautics, Inc., Palm Springs, CA, US, pp. 1–9.

Silva, W.A., Raveh, D.E., 2001. Development of unsteady aerodynamic state-space models from CFD-based pulse responses. In: 42nd AIAA/ASME/ASCE/AHS/ASC Structures Structural Dynamics, and Materials Conference and Exhibit. AIAA-2001-1213, American Institute of Aeronautics & Astronautic, Seattle, WA, US, pp. 1–9.

Smith, T.A., Hakanson, J.W., Nair, S.S., Yurkovich, R.N., 2004. State-space model generation for flexible aircraft. J. Aircr. 41 (6), 1473–1481. http://dx.doi.org/10.2514/1.14433, arXiv:https://doi.org/10.2514/1.14433.

Theodorsen, T., 1935. General Theory of Aerodynamic Instability and the Mechanism of Flutter, Vol. 13. NACA Rept. 496, pp. 374–387.